Bol. Soc. Paran. Mat.
©SPM – E-ISSN-2175-1188
SPM: www.spm.uem.br/bspm

(3s.) **v. 2026 (44)** : 1–28.
ISSN-0037-8712
doi:10.5269/bspm.79551

Dynamical Analysis of Malaria Transmission with Temporary Immunity and Fuzzy Parameters through Mathematical Modeling

Sakshi Singh, Shashank Goel and Alka Tripathi

ABSTRACT: Malaria is one of the most prevalent mosquito-borne diseases across the globe, which is contracted through an Anopheles mosquito bite and continues to pose a major threat to human health in tropical and subtropical regions of the world. The vaccine for malaria has not been developed yet to provide full immunity from the infection of the disease. So, the spread of malaria can be reduced by effective treatment and monitoring the duration of immunity in the recovered individual. In view of this, to examine the dynamics of malaria transmission, we incorporated fuzzy theory to account for the uncertainty in disease dynamics caused by fluctuations in viral loads. Thus, the novel fuzzy SIRSI compartmental epidemic model for malaria disease transmission has been proposed, including the rate of disease transmission, rate of acquired temporary immunity, and rate of disease-induced mortality as functions of the viral load. The positivity and boundedness of the epidemic model have been established. A mathematical analysis of the epidemic model has been conducted, where equilibrium points, basic reproduction number, and fuzzy basic reproduction number have been obtained, and stability analysis for equilibrium points has been performed. The bifurcation threshold formula for viral load has been derived. Also, fuzzy global stability has been carried out by using the approach of graph theory. Numerical simulations have been performed to verify the analytical findings of the epidemic model. Latin hypercube sampling and partial rank correlation coefficients have been used to perform global sensitivity analysis for the basic reproduction number. These results emphasize the need for policymakers and public health professionals to put preventative measures into place to control the spread of malaria in society when disease dynamics are ambiguous.

Keywords: Fuzzy epidemic model, viral load, fuzzy global stability.

Contents

1. Introduction

Malaria is a vector-borne disease that is caused by the protozoan genus Plasmodium: Plasmodium Vivax, Plasmodium Falciparum, Plasmodium Malaria, Plasmodium Ovale and Plasmodium Knowlesi [11]. Out of these five categories, Plasmodium Vivax and Falciparum are considered to be the most dangerous protozoans. An infected Anopheles mosquito bites the person and injects a parasite called sporozoites, which then settles in the hepatocytes (liver cells), where they multiply asexually to form merozoites. These merozoites are released into the bloodstream when the infected liver cells rupture. Once in the blood, the merozoites invade erythrocytes (red blood cells) and continue to multiply until the host cell bursts. This cyclical destruction of red blood cells leads to recurring symptoms such as chills, fever, and sweating [20].

Malaria is a chronic illness that imposes a substantial social, economic, and health burden. Despite being studied for centuries, it remains a major public health challenge. According to the WHO Malaria report 2024 [55], nearly 263 million malaria cases were estimated worldwide in 2023. This represents an increase of 11 million cases over 2022. In the 108 countries where malaria was prevalent in 2000, the expected yearly number of malaria cases stayed constant between 2000 and 2019, ranging between 227 million and 248 million. Further, malaria cases have been rising gradually since 2020, with the majority of this rise occurring in nations in the WHO Eastern Mediterranean Region (15.5%) and the WHO African Region (89.7%). Ethiopia was the primary nation responsible for the rise in cases (+4.5 million) between 2022 and 2023.

The World Health Organization (WHO) has approved numerous control measures that target Anopheles mosquitoes such as indoor residual spray (IRS), long-lasting insecticide-treated nets (LLINs), lotions, and house nets but malaria is still a burden for human society. The intended impact on malaria prevention has been hampered by several factors, including non-adherence, treatment failure, resistance to insecticide, low public knowledge, and household related restriction, despite efforts involving community participation, prompt diagnosis, drug treatment, and disease surveillance [2].

Immunity is the body's natural defense system that protects against harmful pathogens such as bacteria, viruses, and parasites. It involves a complex network of cells, tissues, and organs that work together to identify and eliminate foreign invaders. Immunity to a disease can be acquired at birth by vaccination, infection, or maternal antibodies (for infants born to immune mothers). It must be increased through immunization or infection exposure, but it diminishes with time. Malaria disease incidence tends to decrease consistently with age, meaning that children in the 5–9 age group have noticeably fewer episodes than those in the 1–4 age group [32].

In regions of Africa where malaria has been common for a long time, people get infected so often that they gain some immunity to the disease and may become asymptomatic carriers of the infection [3]. They may have liver and spleen enlargement due to persistent infection as a result of extensive malaria exposure. Sterile immunity is probably never achieved by this gradual process, which might take years or decades to develop [19]. Low-level infection exposure, on the other hand, is crucial because it serves as a vaccination and builds disease resistance [16]. People who use mosquito nets at night, for instance, are typically immune to the disease because the few bites they get outside the nets are insufficient to spread it; instead, the brief exposure to infection builds immunity. Humans are therefore vulnerable to reinfections since their immune systems may not be completely protected (partial immunity) or may gradually deteriorate (temporary immunity).

Over the years, mathematical modeling has been used to understand how infectious illnesses propagate within a population. The first deterministic SIR compartmental model was presented by Kermack and McKendrick in 1927 [21], which sparked interest in mathematical models that use complex presumptions and methods to comprehend disease dynamics. Additional instances of advancements in the field of compartmental epidemic models include a vaccination method in an SIR model [45], a vertical transmission SEIR model [25], an SIR model that incorporates immigration and age structure [15], a delayed SEIQR model to investigate COVID-19 dynamics [8], and an SDIQR model using migrants who are infected [43].

2020 *Mathematics Subject Classification:* 92D30, 34A07, 34D20, 93C42.
Submitted October 15, 2025. Published March 28, 2026

Working for the Indian Medical Service in the 1890s, Sir Ronald Ross identified the malaria parasite's life cycle in mosquitoes. He was also one of the first to publish a number of studies [41,42] in the early 1900s that used mathematical functions to analyze malaria transmission. The SIR model, put forth by Kermack and Mckendrick [21] in 1927, aided in the development of a mathematical model of infectious diseases. Numerous individuals have been working on this concept with improvements ever since. The SEIRS model is put forth by Ngwa and Shu [37] to investigate the spread of disease between human and mosquito populations. Based on the reproduction number, they presented their findings. The authors of [40] presented a seven-dimensional ordinary differential equation model of human-mosquito transmission of Plasmodium falciparum malaria, including nonlinear infectivity as saturation incidence. The authors of [24] employed simple stage-structured mosquito populations and metamorphic stages in their populations. Researchers examine SEIR models with transient immunity and non-linear saturation occurrence in [22]. Over time, numerous researchers have also been using mathematical modeling for the dynamic analysis of malaria transmission.

Connection to existing work and motivation: In 2011, a statistical modeling approach to malaria was introduced by Mandal et al. [30]. In 2012, Chitnis et al. [10] concentrated on modeling mosquito-borne malaria transmission. In 2013, Ghosh [17] created a malaria model that included elements of treatment function. In 2017, Osman et al. [35] presented a transmission SEIR model and applied it to malaria transmission between mosquitoes and humans. Traoré et al. [49] investigated malaria transmission while taking seasonality into account and organized vector populations. In 2018, a model involving two age groups in the human population was created by Beretta et al. [7], whereas Bakary et al. [4] investigated malaria in a periodic context. Olabisi et al. [39] examined the asymptotic stability of a malaria model, and Koutou et al. [23] looked at human population transmission, and a thorough analysis of the literature on malaria modeling was presented by Eikenberry [14]. In 2019, White et al. [54] concentrated on designing model-based strategies for the eradication of malaria. In 2020, Demasse et al. [13] made a contribution to the analysis of malaria transmission, and in a different study, Traoré et al. [48] analyzed the spread of malaria while taking variable temperature and mosquito population. The scope was expanded in 2021 by Tchoumi et al. [46] to incorporate optimal management in situations where COVID-19 and malaria co-infect. A mathematical model was developed by Nwankwo et al. [38] in 2022 to study malaria population dynamics with a focus on temperature-dependent control strategies. A mathematical model was proposed by Tchoumi et al. [47] in 2023 to examine the relationship between childhood malnutrition and malaria. In 2024, Haringo et al. [18] developed a mathematical model of malaria transmission that takes into account treatment interventions and media awareness. Lastly, in 2025, a unique malaria transmission model that incorporates socioeconomic structure into disease dynamics is presented in this work by Ullah et al. [51].

The authors [50] presented vital (birth and death) dynamics in both mosquito and human populations. Since immunization to malaria requires ongoing exposure to reinfection, infected persons either develop some immunity or become susceptible once again. The disease may potentially cause them to pass away. Therefore, the susceptible-infective-immune SIRS in the human population and SI for the mosquito vector population served as the foundation for the model. The pace at which parasites were removed from the human host as a result of treatment was known as the recovery rate. In order to investigate the dynamics of malaria over extended periods of time, the authors developed an endemic model, where vulnerable humans were renewed as a result of births and immunity loss. To re-enter the vulnerable class, the authors included both immune humans who have lost their immunity to the disease and some diseased humans who recovered from infection. There was no vertical transmission, and all newborns were vulnerable to the transmission. Thus, the proposed model in [50] is as follows:

$$\begin{aligned}
\frac{dS_H}{dt} &= \lambda_h N_H - \frac{abS_H I_V}{N_H} + \nu I_H + \gamma R_H - \mu_h S_H \\
\frac{dI_H}{dt} &= \frac{abS_H I_V}{N_H} - \nu I_H - rI_H - \delta I_H - \mu_h I_H \\
\frac{dR_H}{dt} &= rI_H - \gamma R_H - \mu_h R_H
\end{aligned} \tag{1.1}$$

$$\frac{dS_V}{dt} = \lambda_v N_V - \frac{acS_V I_H}{N_H} - \mu_v S_V$$
$$\frac{dI_V}{dt} = \frac{acS_V I_H}{N_H} - \mu_v I_V$$

where the susceptible humans, infected humans, partial immune humans, susceptible mosquitoes, and infected mosquitoes in a society at time t are represented by $S_H(t)$, $I_H(t)$, $R_H(t)$, $S_V(t)$, and $I_V(t)$, respectively. The following is a description of the parameters used in the model system (1.1) and their significance: N_H: total human population, N_V: total mosquito population, a: the average daily biting rate on man by a single mosquito (infection rate), b: the proportion of bites on man that produce an infection, c: the probability that a mosquito becomes infectious, γ: the per capita rate of loss of immunity in human hosts, r: the rate at which human hosts acquire immunity, δ: the per capita death rate of infected human hosts due to the disease, ν: the rate of recovery of human hosts from the disease, λ_h: the per capita natural birth rate of humans, λ_v: the per capita natural birth rate of the mosquitoes, μ_h: the per capita natural death rate of the humans, μ_v: the per capita natural death rate of the mosquitoes.

Now, the natural question arises here that 'What is the effect of the parameters on the dynamics of the disease when the parameters become uncertain?'. To answer this question, DE Barros et al. [5] created SI compartmental models with a fuzzy transmission parameter to account for heterogeneity. Fuzzy theory has been used in a growing number of mathematical models in recent years to describe uncertain processes. Fuzzy parameters were used by Bassanezi and De Barros [6] to address an ecological model. Massad et al. [33] provided studies investigating the use of fuzzy theory in epidemiology, which was the advancement in the field of fuzzy epidemic models. As a result of the developments, models like a fuzzy epidemic model for worm transmission in a computer network have been created (Mishra and Pandey [34]), fuzzy disease transmission and treatment rates in a SIS model (Mondal et al. [36]), a fuzzy SIR model that has an asymptotic transmission rate [53], fuzzy uncertainty is incorporated into an ecological model (Das et al. [12]) and a model of an epidemic that treats fuzzy impreciseness (Mahato et al. [29]). A fuzzy SIR model for COVID-19 dissemination in Indonesia was presented by Abdy et al. [1], taking recovery rates, disease-induced mortality, and disease transmission as fuzzy factors. Therefore, we incorporated Zadeh's [56] fuzzy theory into model (1.1), which allows us to depict the uncertainity of the parameters that play a significant role of disease's propogation in the society . Hence, we propose a fuzzy SIRSI model with temporary immunity of Malaria transmission as described in section 2.

2. Mathematical Model

The human population $N(t)$ is divided into three mutually exclusive compartments: $S(t)$, $I(t)$, and $R(t)$ denote the class of susceptible human population at time t, the class of infected human population at time t, and the class of temporarily immune human population at time t, respectively. The mosquito vector population $N_V(t)$ is also divided into two compartments, $S_V(t)$ and $I_V(t)$, which signify the number of susceptible mosquito vectors at time t and the number of infected mosquito vectors at time t, respectively.

The model formulation and the flowchart (shown in fig.1), capturing the movement of human population and mosquito population in the sub-compartments, are given below:

$$\begin{aligned}
\frac{dS}{dt} &= \Lambda - \frac{\beta(\varrho) S I_V}{N} + \alpha I + \gamma R - \mu S, \\
\frac{dI}{dt} &= \frac{\beta(\varrho) S I_V}{N} - (\alpha + r(\varrho) + \delta(\varrho) + \mu) I, \\
\frac{dR}{dt} &= r(\varrho) I - (\gamma + \mu) R, \\
\frac{dS_V}{dt} &= \Lambda_V - \frac{\psi S_V I}{N} - \mu_V S_V, \\
\frac{dI_V}{dt} &= \frac{\psi S_V I}{N} - \mu_V I_V,
\end{aligned} \tag{2.1}$$

The description of the parameters of the system (2.1) is given in Table 1.

Table 1: Description of parameters of the model (2.1)

Parameter	Interpretation
ψ	Transmission rate from infected human to susceptible mosquito
γ	Rate of loss of temporary immunity in human hosts
α	Recovery rate of human hosts from the disease without immunity
Λ	Natural birth rate of humans
Λ_V	Natural birth rate of the mosquitoes
μ	Natural death rate of humans
μ_V	Natural death rate of the mosquitoes

Since the chances of transmission of the disease from one individual to the other would be increased if the viral load is present higher in the system, the recovery of individuals declines accordingly. As a result, the transmission rate from infected mosquito to susceptible human β, the temporary immunity rate of recovered individual r, and the induced death rate δ are taken as functions of viral load ϱ. Thus, the parameters $\beta(\varrho)$, $r(\varrho)$, and $\delta(\varrho)$ are defined as the membership functions of viral load ϱ [5, 53], which are explained in the subsections (2.1), (2.2), and (2.3), respectively. The following assumptions are considered to derive the model (2.1):

- All parameters described in Table 1 are positive.
- Malaria transmission begins when an infectious Anopheles mosquito bites a individual person.
- Bites from an infected Anopheles mosquito on an already infected people are disregarded.
- Mosquitoes bite to individual at random, regardless of the hosts' infection status.
- Recovered individuals after treatment acquire temporary immunity, which may wane over time, making them susceptible to reinfection.
- All newborns enter the population as susceptible individuals, with no vertical transmission (transmission of infection from infectious mother to new born child).
- Mosquitoes do not recover from infection; instead, the infection is resolved only through the death of the infected individuals.
- The total populations of both humans and mosquitoes are allowed to vary over time.

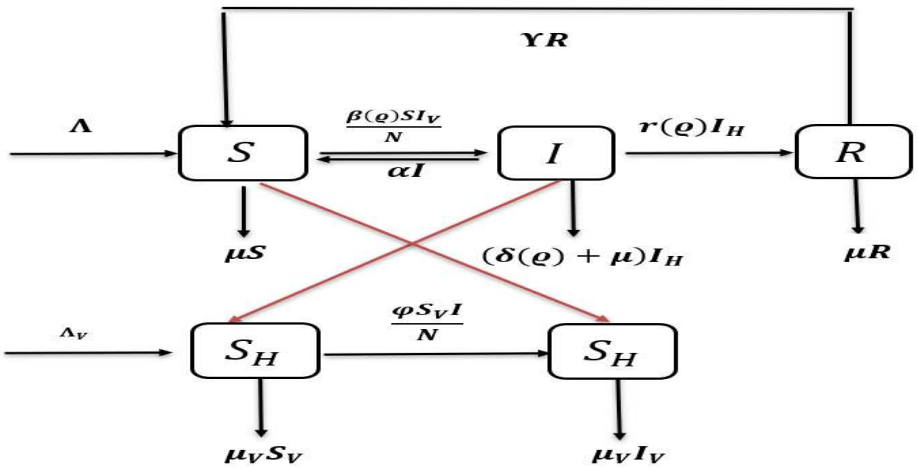

Figure 1: Schematic diagram of Fuzzy SIR-SI Malaria Model (2.1).

2.1. Membership function of the transmission rate from infected mosquito to susceptible human ($\beta(\varrho)$)

The fuzzy membership function for transmission rate $\beta(\varrho)$ was introduced by L.C. de Barros [5] in the epidemic model, which is defined as follows:

$$\beta(\varrho) = \begin{cases} 0, & \text{if } \varrho \leq \varrho_{min} \\ \dfrac{\varrho - \varrho_{min}}{\varrho_M - \varrho_{min}}, & \text{if } \varrho_{min} < \varrho \leq \varrho_M, \\ 1, & \text{if } \varrho_M < \varrho \leq \varrho_{max}. \end{cases} \tag{2.2}$$

The membership function (2.2) is defined that the possibility of transmission from infected mosquito to susceptible human is negligible when the parasite load is less than or equal to ϱ_{min}. In other words, a minimum quantity of parasites is required for malaria transmission to occur. When the parasite load ϱ lies within the range $[\varrho_M, \varrho_{max}]$ the probability of transmission reaches its maximum. Additionally, for parasite levels between ϱ_{min} and ϱ_M, there is a moderate chance of transmission. The membership function describing the $\beta(\varrho)$ is illustrated in fig. 2a.

2.2. Membership function of the disease-induced death rate ($\delta(\varrho)$)

The function $\delta(\varrho)$ increases with the viral load ϱ, as a higher viral load corresponds to a greater likelihood of succumbing to the infectious disease. It reaches its maximum value of $1 - \eta$ at a specific viral load level, denoted by ϱ_M. This membership function, depicted in fig. 2b, is defined [53] as follows:

$$\delta(\varrho) = \begin{cases} \dfrac{(1-\eta) - \delta_0}{\varrho_M}\varrho + \delta_0, & \text{if } 0 \leq \varrho \leq \varrho_M, \\ 1 - \eta, & \text{if } \varrho > \varrho_M. \end{cases} \tag{2.3}$$

2.3. Membership function of rate at which humans acquire temporary immunity ($r(\varrho)$)

Unlike the preceding two membership functions, the rate at which humans acquire temporary immunity decreases with increasing amounts of viral load ϱ. Thus, this behavior arises from the inverse relationship between the temporary immunity rate and viral load. As the viral load in an infected individual rises, the probability of temporary immunity from the disease correspondingly declines. The

membership function displayed in fig. 2c is defined [53] as follows:

$$r(\varrho) = \begin{cases} \dfrac{(r_0 - 1)\varrho}{\varrho_M} + 1, & \text{if } , 0 \leq \varrho \leq \varrho_M, \\ r_0, & \text{if } \varrho > \varrho_M. \end{cases} \tag{2.4}$$

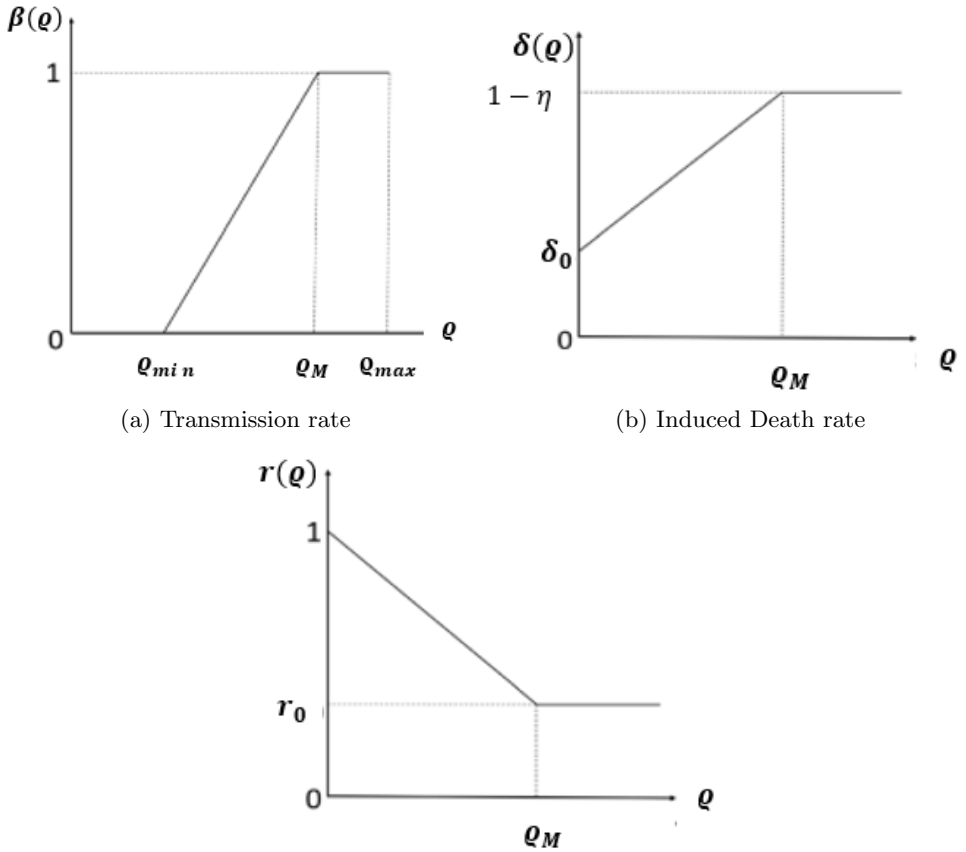

(a) Transmission rate

(b) Induced Death rate

(c) Temporary immunity rate

Figure 2: Membership functions of model (2.1).

2.4. Non-Negativity and boundedness of the solutions

At the boundary $S = 0$, we have

$$\frac{dS}{dt} = \Lambda + \alpha I + \gamma R.$$

- Case 1: $I > 0$, $R > 0$ then $\dfrac{dS}{dt} > 0$.
- Case 2: $I = 0$, $R > 0$ then $\dfrac{dS}{dt} > 0$.
- Case 3: $I > 0$, $R = 0$ then $\dfrac{dS}{dt} > 0$.

Thus, in each cases, we get $\dfrac{dS}{dt} > 0$.
Now, at the boundary $I = 0$, we have

$$\frac{dI}{dt} = \frac{\beta(\varrho) S I_V}{N}.$$

- Case 1: If $S > 0$ and $I_V > 0$ then $\dfrac{dI}{dt} > 0$.
- Case 2: If $S > 0$ and $I_V = 0$ then $\dfrac{dI}{dt} = 0$.
- Case 3: If $S = 0$ and $I_V > 0$ then $\dfrac{dI}{dt} = 0$.

Thus, in each of these cases, we get $\dfrac{dI}{dt} \geq 0$.
And, at the boundary $R = 0$, we have

$$\frac{dR}{dt} = rI.$$

- Case 1: If $I > 0$ then $\dfrac{dR}{dt} > 0$.
- Case 2: If $I = 0$ then $\dfrac{dR}{dt} = 0$.

Thus, $\dfrac{dR}{dt} \geq 0$. In a similar way, one can also check the non-negativity of $S_V(t)$ and $I_V(t)$.

Now, we determine the boundedness of the solution of model (2.1).

Let the population function of host $N(t)$ at any time t be given as

$$N(t) = S(t) + I(t) + R(t). \tag{2.5}$$

Differentiating (2.5) and using (2.1), we obtain

$$\frac{dN}{dt} = \Lambda - \mu N(t) - \delta I(t).$$

Since $I(t) \leq N(t)$ and $I(t) > 0 \; \forall \; t > 0$, therefore we get

$$\Lambda - (\mu + \delta)N(t) \leq \frac{dN}{dt} \leq \Lambda - \mu N(t). \tag{2.6}$$

On integrating (2.6) and taking limit as $t \to \infty$, we obtain

$$\frac{\Lambda}{\mu + \delta} \leq \lim_{t \to \infty} N(t) \leq \frac{\Lambda}{\mu}.$$

Similarly,

$$\lim_{t \to \infty} N_V(t) \leq \frac{\Lambda_V}{\mu_V}.$$

Therefore, a feasible region κ will be given below to analyze system (2.1), where

$$\kappa = \left\{ (S, I, R, S_V, I_V) \in \mathbb{R}^5_+ : 0 \leq S + I + R \leq \frac{\Lambda}{\mu} \text{ and } 0 \leq S_V + I_V \leq \frac{\Lambda_V}{\mu_V} \right\}.$$

From the above explanation, we have the following theorem:

Theorem 2.1 *The feasible region κ is positively invariant for the system (2.1).*

3. Mathematical Analysis of the Model

Since $S + I + R = N$ and $S_V + I_V = N_V$, we consider following system for the stability analysis of the model (2.1):

$$\begin{aligned}
\frac{dN}{dt} &= \Lambda - \mu N - \delta(\varrho) I, \\
\frac{dI}{dt} &= \beta(\varrho)(N - I - R)\frac{I_V}{N} - (\alpha + r(\varrho) + \delta(\varrho) + \mu) I, \\
\frac{dR}{dt} &= r(\varrho) I - (\gamma + \mu) R, \\
\frac{dN_V}{dt} &= \Lambda_V - \psi(N_V - I_V)\frac{I}{N} - \mu_V (N_V - I_V), \\
\frac{dI_V}{dt} &= \psi(N_V - I_V)\frac{I}{N} - \mu_V I_V.
\end{aligned} \tag{3.1}$$

3.1. Disease free equilibrium points

The disease free equilibrium point for the system (3.1) is given by:

$$E_0 = (N^0, I^0, R^0, N_V^0, I_V^0) = \left(\frac{\Lambda}{\mu}, 0, 0, \frac{\Lambda_V}{\mu_V}, 0\right).$$

3.2. Basic reproduction number

Now, to find the basic reproduction number, $R_0(\varrho)$, of the model (3.1), we use next generation matrix method [9, 52]. The two matrices $\mathfrak{F}$ and $\mathbb{V}$ from the model (3.1) as follows:

$$\mathfrak{F} = \begin{bmatrix} \beta(\varrho)(N - I - R)\frac{I_V}{N} \\ \psi(N_V - I_V)\frac{I}{N} \end{bmatrix}$$

and

$$\mathbb{V} = \begin{bmatrix} (\alpha + r(\varrho) + \delta(\varrho) + \mu) I \\ \mu_V I_V \end{bmatrix}.$$

Let $\mathcal{F}$ and $\mathcal{V}$ be the Jacobian of the matrices $\mathfrak{F}$ and $\mathbb{V}$ respectively, at the disease free equilibrium point E_0. Then, we get

$$\mathcal{F} = \begin{bmatrix} 0 & \beta(\varrho) \\ \frac{\psi \Lambda_V \mu}{\mu_V \Lambda} & 0 \end{bmatrix}$$

and

$$\mathcal{V} = \begin{bmatrix} (\alpha + r(\varrho) + \delta(\varrho) + \mu) & 0 \\ 0 & \mu_V \end{bmatrix}.$$

The basic reproduction number, $R_0(\varrho)$, is obtained by evaluating the spectral radius of $(\mathcal{F}\mathcal{V}^{-1})$. Then, we get $R_0(\varrho)$ as follows:

$$R_0(\varrho) = \sqrt{\frac{\beta(\varrho)\mu\psi\Lambda_V}{(\alpha + r(\varrho) + \delta(\varrho) + \mu)\mu_V^2 \Lambda}}. \tag{3.2}$$

3.3. Existence of endemic equilibrium point

The endemic equilibrium point of the system (3.1) satisfies the following algebraic equations:

$$\frac{dN}{dt} = 0, \ \frac{dI}{dt} = 0, \ \frac{dR}{dt} = 0, \ \frac{dN_V}{dt} = 0, \ \frac{dI_V}{dt} = 0.$$

Then, the system (3.1) has an endemic equilibrium point $E^*(N^*, I^*, R^*, N_V^*, I_V^*)$, where

$$N^* = \frac{\Lambda - \delta(\varrho) I^*}{\mu}, R^* = \frac{r(\varrho) I^*}{\mu + \gamma}, N_V^* = \frac{\Lambda_V}{\mu_V}, I_V^* = \frac{\psi \Lambda_V I^*}{\mu_V(\psi I^* + \mu_V N^*)},$$

and I^* is the root of the following quadratic equation:

$$f(I) = A_1 I^2 + A_2 I + A_3 = 0, \tag{3.3}$$

where

$$A_1 = \frac{(\alpha + r(\varrho) + \delta(\varrho) + \mu)\delta(\varrho)}{\mu^2}[\psi\mu - \mu_V\delta(\varrho)],$$
$$A_2 = -\frac{\delta(\varrho)}{\mu^2\mu_V}(R_0(\varrho)^2 - 1)(\alpha + r(\varrho) + \delta(\varrho) + \mu)\mu_V^2\Lambda - \frac{\beta(\varrho)\psi\Lambda_V}{\mu_V}\left(1 + \frac{r(\varrho)}{\mu+\gamma}\right) - \frac{(\alpha + r(\varrho) + \delta(\varrho) + \mu)\Lambda}{\mu^2}(\psi\mu - \mu_V\delta(\varrho)),$$
$$A_3 = \frac{\Lambda^2\mu_V(\alpha + r(\varrho) + \delta(\varrho) + \mu)(R_0(\varrho)^2 - 1)}{\mu^2}.$$

For N^* to be positive, we need $I^* < \dfrac{\Lambda}{\delta(\varrho)}$. So, we consider the range of I as $0 < I < \dfrac{\Lambda}{\delta(\varrho)}$ to find the root of the equation (3.3).

Since A_1 is positive for $\psi\mu > \mu_v\delta(\varrho)$ and

$$f(0) = A_3 = \frac{\Lambda^2\mu_V(\alpha + r(\varrho) + \delta(\varrho) + \mu)(R_0(\varrho)^2 - 1)}{\mu^2},\ f\left(\frac{\Lambda}{\delta(\varrho)}\right) = A_4 = -\frac{\Lambda}{\delta(\varrho)}\left[\frac{\beta(\varrho)\psi\Lambda_V}{\mu_V}\left(1 + \frac{r(\varrho)}{\mu+\gamma}\right)\right].$$

Now, $f\left(\dfrac{\Lambda}{\delta(\varrho)}\right) < 0$ and $f(0) > 0$ for $R_0(\varrho) > 1$. Since the equation (3.3) is quadratic, so it has atmost two roots that lie between $0 < I < \dfrac{\Lambda}{\delta(\varrho)}$ and must have a unique positive root for $R_0(\varrho) > 1$.

When $R_0(\varrho) < 1$, $f(0) < 0$ and $f\left(\dfrac{\Lambda}{\delta(\varrho)}\right) < 0$. So, there is probability of two positive roots or no roots of the equation (3.3) in the interval $\left(0, \dfrac{\Lambda}{\delta(\varrho)}\right)$. But, since $A_1 > 0$ and $A_3 < 0$ for $R_0(\varrho) < 1$ and thus by applying the Descartes rule of signs, there is a unique positive root of equation (3.3) which contradicts the existence of two positive roots in the interval $\left(0, \dfrac{\Lambda}{\delta(\varrho)}\right)$.

Therefore, it can be established that there is no positive root of the equation (3.3) lying between 0 and $\dfrac{\Lambda}{\delta(\varrho)}$ when $R_0(\varrho) < 1$ and there is a unique positive root for $R_0(\varrho) > 1$.

3.4. Fuzzy basic reproduction number $R_0^f(\varrho)$

The basic reproduction number $R_0(\varrho)$ depends on the parasitic viral load ϱ. Now, we investigate that how $R_0(\varrho)$ varies with different amount of viral load.

Case 1: When $\varrho \le \varrho_{min}$, then $\beta(\varrho) = 0$, $r(\varrho) > 0$ and $\delta(\varrho) > 0$. Under these conditions, $R_0(\varrho) = 0$, indicating that malaria is not present in the population. Consequently, the disease is eliminated.

Case 2: When $\varrho_{min} < \varrho \le \varrho_M$, then $\beta(\varrho) = \dfrac{\varrho - \varrho_{min}}{\varrho_M - \varrho_{min}}$, $r(\varrho) > 0$ and $\delta(\varrho) > 0$. Thus the basic reproduction number is as follows:

$$0 < R_0(\varrho) \equiv \sqrt{\left(\frac{\varrho - \varrho_{min}}{\varrho_M - \varrho_{min}}\right)\frac{\psi\Lambda_V\mu}{(\alpha + r(\varrho) + \delta(\varrho) + \mu)\mu_V^2\Lambda}}.$$

Case 3: When $\varrho_M < \varrho \le \varrho_{max}$, then $\beta(\varrho) = 1$, $r(\varrho) > 0$ and $\delta(\varrho) > 0$. Thus the basic reproduction number is as follows:

$$0 < R_0(\varrho) \le \sqrt{\frac{\psi\Lambda_V\mu}{(\alpha + r(\varrho) + \delta(\varrho) + \mu)\mu_V^2\Lambda}}.$$

So, we observe that the $R_0(\varrho)$ increases as the parasitic viral load ϱ increases (as shown fig. 5) and also a bounded function with a finite upper bound $\sqrt{\dfrac{\psi\Lambda_V\mu}{(\alpha + r(\varrho) + \delta(\varrho) + \mu)\mu_V^2\Lambda}} > 0$. Therefore, $R_0(\varrho)$ can be

considered as a fuzzy variable, and its expected value, represented by $E[R_0(\varrho)]$, is also be well-defined. The fuzzy number $R_0(\varrho)$ is given as:

$$R_0(\varrho) = \left(0,\ \sqrt{\left(\frac{\varrho-\varrho_{min}}{\varrho_M-\varrho_{min}}\right)\frac{\psi\mu\Lambda_V}{(\alpha+r(\varrho)+\delta(\varrho)+\mu)\mu_V^2\Lambda}},\ \sqrt{\frac{\psi\mu\Lambda_V}{(\alpha+r(\varrho)+\delta(\varrho)+\mu)\mu_V^2\Lambda}}\right),$$

which is characterized as a triangular fuzzy number. Thus, fuzzy basic reproduction number $R_0^f(\varrho)$ for the above triangular fuzzy number $R_0(\varrho)$ can be obtained on the similar argument of using expected value of fuzzy variable as introduced by B. Liu and Y.-K. Liu in [26, 27, 28].

Proposition 1 (Fuzzy basic reproduction number, $(R_0^f(\varrho))$: The fuzzy basic reproduction number $R_0^f(\varrho)$ for the model (2.1) is defined as:

$$\begin{aligned} R_0^f(\varrho) &= E[R_0(\varrho)] \\ &= \frac{1}{4}\left(2\sqrt{\frac{\varrho-\varrho_{min}}{\varrho_M-\varrho_{min}}}+1\right)\sqrt{\frac{\psi\mu\Lambda_V}{(\alpha+r(\varrho)+\delta(\varrho)+\mu)\mu_V^2\Lambda}},\ \text{for } \varrho>\varrho_{min}. \end{aligned}$$

Here, $E[.]$ represents the expected value of a fuzzy number.

3.5. Bifurcation Threshold Formula for Viral Load (ϱ^*)

The bifurcation point of model (3.1) is provided by the condition $R_0(\varrho^*)=1$. In this subsection, our goal is to identify a critical viral load value ϱ^* such that $R_0(\varrho)>1$ for all $\varrho>\varrho^*$ and $R_0(\varrho)<1$ for all $\varrho<\varrho^*$. Since equation (3.2) shows that $R_0(\varrho)$ depends on ϱ, we adopt the approach used by [1] and treat ϱ^* as the bifurcation point of model (3.1).
By setting equation (3.2) equal to 1, we derive:

$$(r(\varrho)+\alpha+\delta(\varrho)+\mu)\mu_V^2\Lambda=\beta(\varrho)\psi\Lambda_V. \tag{3.4}$$

Substituting the membership function expressions from (2.2), (2.3), (2.4) into (3.4), we obtain the following expression for ϱ^*:

$$\varrho^*=\frac{\varrho_M\varrho_{min}\psi\Lambda_V\mu+\varrho_M(\varrho_M-\varrho_{min})\Lambda\mu_V^2(1+\alpha+\delta_0+\mu)}{\varrho_M\psi\Lambda_V\mu-\Lambda\mu_V^2(\varrho_M-\varrho_{min})(a-\delta_0-n)}. \tag{3.5}$$

3.6. Local Stability

Theorem 3.1 *At the disease-free equilibrium point E_0, the system is asymptotically stable when $R_0(\varrho)<1$ and is unstable when $R_0(\varrho)>1$.*

Proof: For the system (3.1), the Jacobian matrix J_1 at disease free equilibrium point $E_0(N^0,0,0,0,N_V^0,0)$ is as follows:

$$J_1=\begin{bmatrix} -\mu & -\delta(\varrho) & 0 & 0 & 0 \\ 0 & -(\alpha+r(\varrho)+\delta(\varrho)+\mu) & 0 & 0 & \beta(\varrho) \\ 0 & r(\varrho) & -(\gamma+\mu) & 0 & 0 \\ 0 & -\dfrac{\psi\Lambda_V\mu}{\mu_V\Lambda} & 0 & -\mu_V & \mu_V \\ 0 & \dfrac{\psi\Lambda_V\mu}{\mu_V\Lambda} & 0 & 0 & -\mu_V \end{bmatrix}.$$

The three eigen values of J_1 are $-\mu,-(\gamma+\mu),-\mu_V$ and the remaining eigen values of J_1 are the root of the following quadratic equation:

$$\lambda^2+K_1\lambda+K_2=0, \tag{3.6}$$

where

$$K_1=((\alpha+r(\varrho)+\delta(\varrho)+\mu)+\mu_V) \text{ and } K_2=((\alpha+r(\varrho)+\delta(\varrho)+\mu)\mu_V)(1-R_0^2). \tag{3.7}$$

Since

$$K_1 > 0 \text{ and } K_2 > 0 \text{ for } R_0 < 1,$$

then by Routh-Hurwitz criteria, the equation (3.6) will have negative roots or roots with negative real parts and so the disease free equilibrium point E_0 is locally asysmptotically stable when $R_0(\varrho) < 1$ whereas $K_2 < 0$ for $R_0(\varrho) > 1$ and so consequently, E_0 is unstable when $R_0(\varrho) > 1$.

Theorem 3.2 *The endemic equilibrium point E^* of model (3.1) is locally asymptotically stable for $R_0(\varrho) > 1$, if the following conditions are satisfied:*

1. $X_1 > 0$,
2. $X_4 > 0$,
3. $X_1X_2 - X_3 > 0$,
4. $X_1X_2X_3 - X_3^2 - X_4X_1^2 > 0$,

where $X_i, i = 1, 2, 3, 4$ are stated in proof of the theorem.

Proof: The Jacobian matrix J_2 of system (3.1) evaluated at the endemic equilibrium point $E^*(N^*, I^*, R^*, N_V^*, I_V^*)$ can be expressed as follows:

$$J_2 = \begin{bmatrix} -\mu & -\delta(\varrho) & 0 & 0 & 0 \\ 0 & -a_{22} & -a_{23} & 0 & a_{25} \\ 0 & r(\varrho) & -(\gamma+\mu) & 0 & 0 \\ a_{41} & a_{42} & 0 & -a_{44} & a_{44} \\ a_{51} & a_{52} & 0 & a_{54} & -a_{44} \end{bmatrix}$$

where,

$$a_{21} = \beta(\varrho)\left[\frac{I^*}{N^{*2}} + \frac{R^*}{N^{*2}}\right] I_V^* \ , \ a_{22} = \frac{\beta(\varrho)I_V^*}{N^*} + (\alpha + r(\varrho) + \delta(\varrho) + \mu) \ , \ a_{23} = \frac{\beta(\varrho)I_V^*}{N^*} \ ,$$

$$a_{25} = \frac{\beta(\varrho)(N^* - I^* - R^*)}{N^*}$$

$$a_{41} = \psi\left[\frac{N_V^*}{N^{*2}} - \frac{I_V^*}{N^{*2}}\right] I^* \ , \ a_{42} = \frac{\psi}{N^*}[I_V^* - N_V^*] \ , \ a_{44} = \frac{\psi I^*}{N^*} + \mu_V \ , \ a_{51} = \frac{\psi(I_V^* - N_V^*)I^*}{N^{*2}}$$

$$a_{52} = \frac{\psi(N_V^* - I_V^*)}{N^*} \ , \ a_{54} = \frac{\psi I^*}{N^*}.$$

The one eigen value of J_2 is $-\mu_V$ and remaining eigen values are the root of the biquadratic equation given as follows:

$$\lambda^4 + X_1\lambda^3 + X_2\lambda^2 + X_3\lambda + X_4 = 0, \tag{3.8}$$

where

$$\begin{aligned} X_1 &= a_{22} + 2a_{44} + \gamma + \mu, \\ X_2 &= 2a_{22}a_{44} + a_{44}^2 - a_{25}a_{52} - a_{44}a_{54} + a_{23}r + a_{22}(\gamma+\mu) + 2a_{44}(\gamma+\mu), \\ X_3 &= a_{22}a_{44}^2 - a_{25}a_{44}a_{52} - a_{25}a_{42}a_{54} - a_{22}a_{44}a_{54} + 2a_{23}a_{44}r + 2a_{22}a_{44}(\gamma+\mu) + a_{44}^2(\gamma+\mu) \\ &\quad - a_{25}a_{52}r - a_{44}a_{54}(\gamma+\mu), \\ X_4 &= a_{23}a_{44}^2 r - a_{23}a_{44}a_{54}r + a_{22}a_{44}^2(\gamma+\mu) - a_{25}a_{44}a_{52}(\gamma+\mu) - a_{25}a_{42}a_{54}(\gamma+\mu) \\ &\quad - a_{22}a_{44}a_{54}(\gamma+\mu). \end{aligned}$$

According to the Routh–Hurwitz criterion, all roots of the biquadratic equation (3.8) will have negative real parts under the following conditions:

$$X_1 > 0, \quad X_4 > 0, \quad X_1X_2 - X_3 > 0, \quad X_1X_2X_3 - X_3^2 - X_4X_1^2 > 0. \tag{3.9}$$

Hence, the endemic equilibrium point E_1 of model (3.1) is locally asymptotically stable for $R_0(\varrho) > 1$ provided the conditions in (3.9) are satisfied.

3.7. Fuzzy Global stability of endemic equilibrium point

Theorem 3.3 *The Endemic Equilibrium $Z^*(S^*, I^*, R^*, S_V^*, I_V^*) \in int\ (\kappa)$ of system (2.1) exhibits global asymptotic stability within the interior of the positively invariant compact set κ when $\varrho > \varrho_{min}$ (i.e $\varrho_{min} < \varrho \leq \varrho_M$ or $\varrho_M < \varrho \leq \varrho_{max}$) and $R_0(\varrho) > 1$.*

Proof: The classical Lyapunov function-based analysis is employed to determine fuzzy global asymptotic stability at the equilibrium point Z^* of the system (2.1). This is a classical graph-theoretical approach introduced by Shuai and Driessche [44]. The Lyapunov function of system (2.1) is constructed as:

$$D_i : \omega \to R,\ i \in \{1, 2, 3, 4, 5\},$$

where

$$D_1 = S - S^* - S^* \ln\left(\frac{S}{S^*}\right),\ D_2 = I - I^* - I^* \ln\left(\frac{I}{I^*}\right),\ D_3 = R - R^* - R^* \ln\left(\frac{R}{R^*}\right),$$
$$D_4 = S_V - S_V^* - S_V^* \ln\left(\frac{S_V}{S_V^*}\right),\ D_5 = I_V - I_V^* - I_V^* \ln\left(\frac{I_V}{I_V^*}\right).$$

The standard inequalities $1 - x + \ln x \leq 0$ and $2 - x - \frac{1}{x} \leq 0$, for $x > 0$ are being used in the differentiation of D_i with respect to t, where $i = 1, 2, 3, 4, 5$.

$$\begin{aligned}
\frac{dD_1}{dt} &= \left(1 - \frac{S^*}{S}\right)\frac{dS}{dt} = \left(1 - \frac{S^*}{S}\right)\left(\Lambda - \frac{\beta(\varrho)SI_V}{N} + \alpha I + \gamma R - \mu S\right) \\
&\leq \frac{\beta(\varrho)I_V^* S^*}{N}\left(\frac{I_V}{I_V^*} - \frac{S^*}{S} - \ln\frac{I_V}{I_V^*} + \ln\frac{S^*}{S}\right) + \gamma R\left(1 - \frac{S^* R}{S R^*} + \frac{S^*}{S} + \frac{R}{R^*}\right) \\
&\leq \frac{\beta(\varrho)I_V^* S^*}{N}\left(\frac{I_V}{I_V^*} - \frac{S^*}{S} - \ln\frac{I_V}{I_V^*} + \ln\frac{S^*}{S}\right) + \gamma R\left(\frac{S^*}{S} + \frac{R}{R^*} - \ln\frac{S^*}{S} - \ln\frac{R}{R^*}\right) \\
&= a_{15}G_{15} + a_{13}G_{13}. \\
\frac{dD_2}{dt} &= \left(1 - \frac{I^*}{I}\right)\frac{dI}{dt} = \left(1 - \frac{I^*}{I}\right)\left(\frac{\beta(\varrho)SI_V}{N} - (\alpha + \delta(\varrho) + r(\varrho) + \mu)I\right) \\
&\leq \frac{\beta(\varrho)I_V^* S^*}{N}\left(\frac{SI_V}{S^* I_V^*} - \frac{I}{I^*} - \ln\frac{SI_V}{S^* I_V^*} - \ln\frac{I^*}{I}\right) = a_{21}G_{21}. \\
\frac{dD_3}{dt} &= \left(1 - \frac{R^*}{R}\right)\frac{\dot{R}}{dt} = \left(1 - \frac{R^*}{R}\right)(rI - (\gamma + \mu)R) \\
&\leq rI^*\left(\frac{I}{I^*} - \frac{R}{R^*} + \ln\frac{R}{R^*} - \ln\frac{I}{I^*}\right) = a_{32}G_{32}.
\end{aligned}$$

$$\begin{aligned}
\frac{dD_4}{dt} &= \left(1 - \frac{S_V^*}{S_V}\right)\dot{S}_V = \left(1 - \frac{S_V^*}{S_V}\right)\left(\Lambda_V - \frac{\psi S_V I}{N} - \mu_V S_V\right) \\
&\leq \frac{\psi I^* S_V^*}{N}\left(\frac{I}{I^*} - \frac{S_V^*}{S_V} - \ln\frac{I}{I^*} - \ln\frac{S_V}{S_V^*}\right) = a_{43}G_{43}. \\
\frac{dD_5}{dt} &= \left(1 - \frac{I_V^*}{I_V}\right)\dot{I}_V = \left(1 - \frac{I_V^*}{I_V}\right)\left(\frac{\psi S_V I}{N} - \mu_V I_V\right) \\
&\leq \frac{\psi S_V^* I^*}{N}\left(\frac{S_V I}{S_V^* I^*} - \frac{I_V}{I_V^*} - \ln\frac{S_V I}{S_V^* I^*} - \ln\frac{I_V^*}{I_V}\right) = a_{54}G_{54}.
\end{aligned}$$

Case 1: If $\varrho \leq \varrho_{min}$, then we have $\beta(\varrho) = 0$ and $r(\varrho) > 0$ and $\delta(\varrho) > 0$ and so $\frac{dD_1}{dt}$ and $\frac{dD_2}{dt}$ become as:

$$\frac{dD_1}{dt} = \gamma R\left(\frac{S^*}{S} + \frac{R}{R^*} - \ln\frac{S^*}{S} - \ln\frac{R}{R^*}\right) = a_{13}G_{13} \text{ and } \frac{dD_2}{dt} = 0.$$

The corresponding weighted directed graph (G, A) is illustrated in fig. 3. Based on this digraph, the conditions of Theorem 3.5 [44] are not satisfied. Consequently, a Lyapunov function for system (2.1) cannot be constructed. Thus, the system (2.1) is not globally asymptotically stable at equilibrium point Z^* when $\varrho \leq \varrho_{min}$.

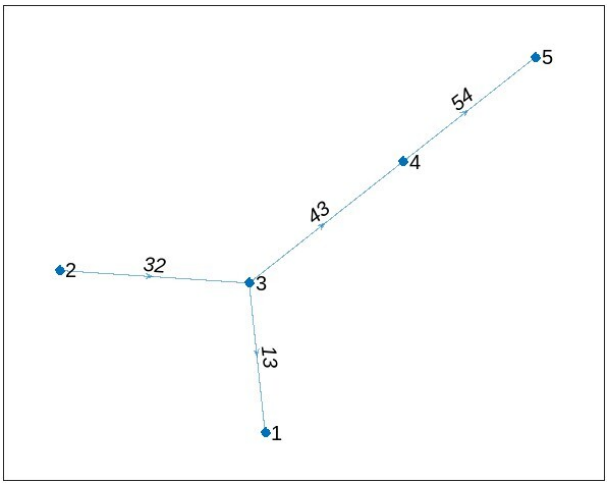

Figure 3: The weighted directed graph (G, A) when $\varrho \leq \varrho_{min}$, where $32 = a_{32}$, $43 = a_{43}$, $54 = a_{54}$ and $13 = a_{13}$.

Case 2: If $\varrho > \varrho_{min}$, (i.e., $\varrho_{min} < \varrho \leq \varrho_M$ or $\varrho_M < \varrho \leq \varrho_{max}$), then we have $\beta(\varrho) > 0$, $r(\varrho) > 0$ and $\delta(\varrho) > 0$. Fig. 4 illustrates the corresponding weighted digraph (G, A) for this case.

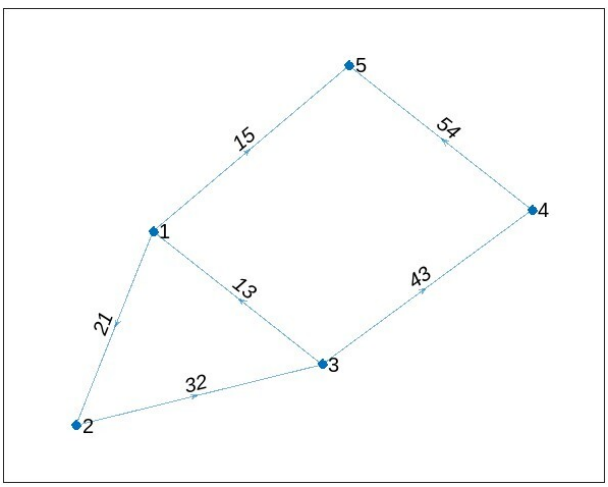

Figure 4: The weighted directed graph (G, A) when $\varrho > \varrho_{min}$, where $21 = a_{21}$, $15 = a_{15}$, $54 = a_{54}$, $43 = a_{43}$, $13 = a_{13}$ and $32 = a_{32}$.

The weights of the digraph are:

$$a_{21} = a_{15} = \frac{\beta(\varrho) I_V^* S^*}{N}, \quad a_{13} = \gamma R,$$

$$a_{32} = rI^*, \quad a_{43} = a_{54} = \frac{\psi S_V^* I^*}{N}.$$

Now, consider the weighted matrix $A = [a_{ij}]_{5\times 5}$, where each element $a_{ij} > 0$ denotes the weight of the arc from node j to node i. It is observed that $G_{51} + G_{45} + G_{34} + G_{31} = 0$ and $G_{12} + G_{31} + G_{23} = 0$.

Thus, digraph satisfies the Theorem 3.5 [44], then there exists $c_i,\ i = 1, 2, 3, 4, 5$, such that

$$L = c_1L_1 + c_2L_2 + c_3L_3 + c_4L_4 + c_5L_5 \tag{3.10}$$

is a Lyapunov function for the system (2.1). The relationships among the values of $c_i,\ i = 1, 2, 3, 4, 5$ are derived (by applying the approach of Theorems 3.3 and 3.4 [44] as follows: $c_1a_{15} = c_5a_{54}$, $c_5a_{54} = c_4a_{41}$, $c_1a_{13} = c_3a_{32}$, $c_2a_{21} = c_3a_{32}$ and $c_4 = 0$. Then, the Lyapunov function L given in (3.10) becomes:

$$L = c_1L_1 + c_2L_2 + c_3L_3 + c_5L_5. \tag{3.11}$$

Thus, the fact that $\dot{L} = c_1\dot{L}_1 + c_2\dot{L}_2 + c_3\dot{L}_3 + c_5\dot{L}_5 \leq 0$ implies $Z = Z^*$. So, the largest invariant set for system (2.1), where $\dfrac{dL}{dt} = 0$ is the singleton set Z^*. This proves the uniqueness and global asymptotic stability of Z^* in the interior of κ under the condition $R_0(\varrho) > 1$.

4. Numerical Results and Simulation

In this section, we carry out numerical simulations of model (2.1) in order to validate our theoretical results.

Table 2: Assumed numerical values or parameters of model (2.1).

Parameters	ψ	γ	α	Λ	Λ_V	μ	μ_V
Baseline/ Values	0.55	0.05	0.002	1000	0.085	0.125	0.002

We use the parametric values provided in table 2 and the range of state variable ϱ is assumed between 10 to 100. The initial values are taken to be as: $S(0) = 1$, $I(0) = 0.5$, $R(0) = 0.25$, $S_V(0) = 2$ and $I_V(0) = 1$. The values of membership functions $\beta(\varrho)$, $\delta(\varrho)$, $r(\varrho)$ and the basic reproduction number $R_0(\varrho)$ for increasing values of ϱ, ranging from ϱ_{min} to ϱ_M (10 and 100, respectively) are given in table 3. Using Eq. (3.5), we calculated the critical viral-load value ϱ^* when $R_0(\varrho) = 1$ and it is found to be approximately 62.465. This evaluation is supported graphically by fig.5 and quantitatively by table 3. Further, fig.5 and table 3 show that $R_0(\varrho)$ falls below 1 for viral-load values below ϱ^* and rises above 1 for viral-load values above ϱ^*.

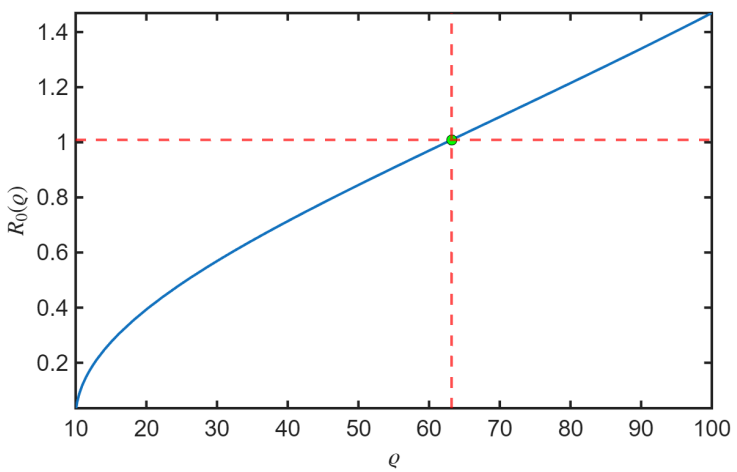

Figure 5: The basic reproduction number $R_0(\varrho)$ w.r.t viral load ϱ.

Table 3: The values of membership functions $\beta(\varrho)$, $r(\varrho)$, $\delta(\varrho)$ and $R_0(\varrho)$ for different values (ranging between 10 to 100) of viral load ϱ.

Simulation	ϱ_{min}	ϱ_M	ϱ	$\beta(\varrho)$	$r(\varrho)$	$\delta(\varrho)$	$R_0(\varrho)$
1	10	100	25	0.1667	0.7625	0.13625	0.487214
2	10	100	45	0.3889	0.5725	0.23325	0.780452
3	10	100	62.465	0.5829	0.4065	0.31795	1.00006
4	10	100	78	0.7556	0.2590	0.3933	1.19014
5	10	100	100	1	0.05	0.5	1.469

The Routh-Hurwitz criteria in Theorem 3.1 for disease free equilibrium point is validated graphically by fig.6 which shows that K_1 and K_2 are positive w.r.t viral load $\varrho < \varrho^*$, i.e, when $R_0(\varrho) < 1$. The fig.7 depicts the stability of model (2.1) at disease free equilibrium point E_0 at $\varrho = 55$ when $R_0(\varrho) < 1$.

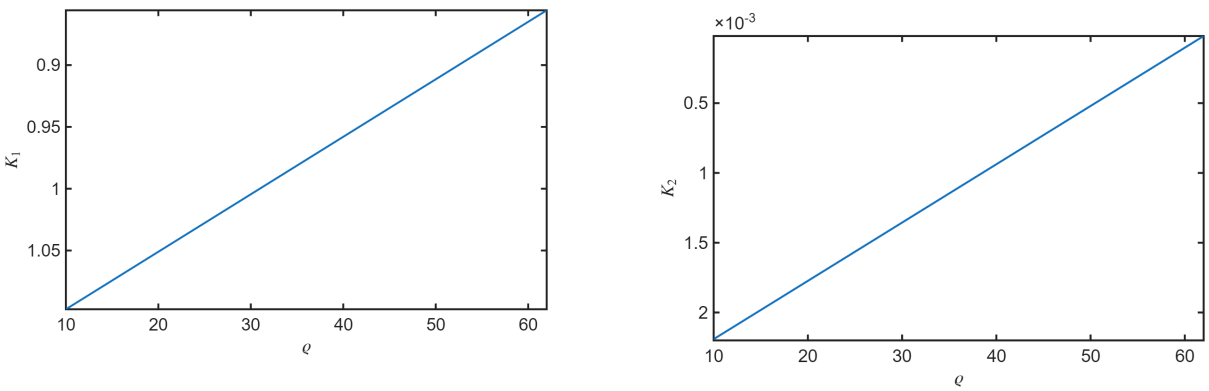

(a) (b)

Figure 6: Routh-Hurwitz conditions for stability at disease free equilibrium points E_0 (Theorem 3.1) (a)K_1 w.r.t viral load ϱ, (b)K_2 w.r.t to viral load ϱ.

In order to ascertain whether or not the endemic equilibrium point E^* is unique when $R_0(\varrho) > 1$ in the interval $\left(0, \frac{\Lambda}{\delta(\varrho)}\right)$, we have determined the values of the coefficients A_1, A_2 and A_3 of the cubic polynomial in Eq.(3.3) and the value of $A_4 = f\left(\frac{\Lambda}{\delta(\varrho)}\right)$. Since A_1 is positive w.r.t the viral load $\varrho > \varrho^* = 62.465$ as shown by fig.9a and A_2 is always negative by the expression given in section 3.3 when $R_0(\varrho) > 1$. It is observed that the value of $A_3(= f(0))$ is positive w.r.t the viral load $\varrho > \varrho^* = 62.465$ when $R_0(\varrho) > 1$ which is depicted by fig.9b. Also, we observed that $A_4 = f\left(\frac{\Lambda}{\delta(\varrho)}\right)$ is negative w.r.t the viral load $\varrho > \varrho^* = 62.465$ which is depicted by fig.9c when $R_0(\varrho) > 1$. Therefore, the endemic equilibrium point E^* is unique in the interval $\left(0, \frac{\Lambda}{\delta(\varrho)}\right)$ when $R_0(\varrho) > 1$. The model (3.1) exhibits forward bifurcation shown by fig.8 (when $\Lambda = 10$ and other parameters are taken as table 2).

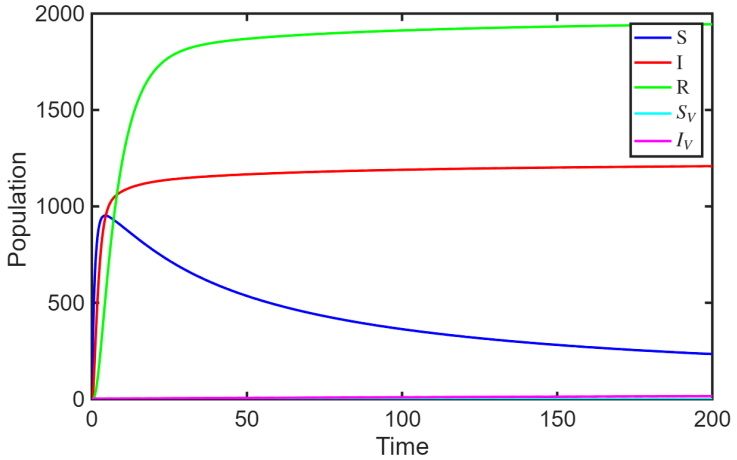

Figure 7: The graph shows the stable behaviour of epidemic model (2.1) around the disease-free equlibrium point E_0 w.r.t time when $R_0(\varrho) = 0.8614 < 1$ (at $\varrho = 55$).

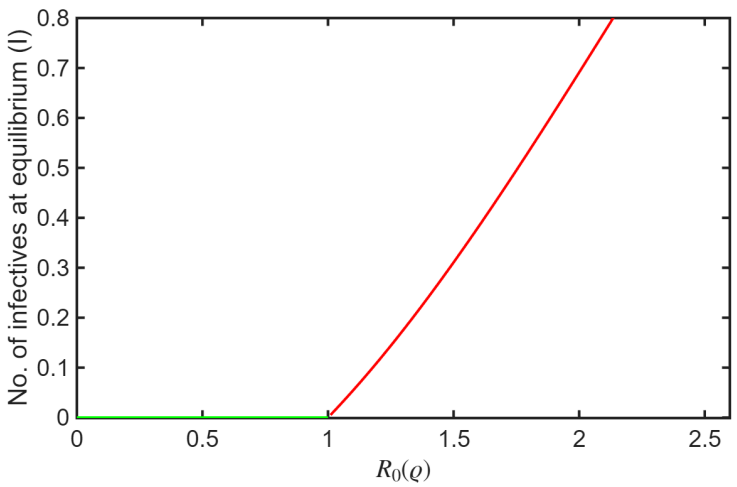

Figure 8: Forward Bifurcation for the model (3.1)

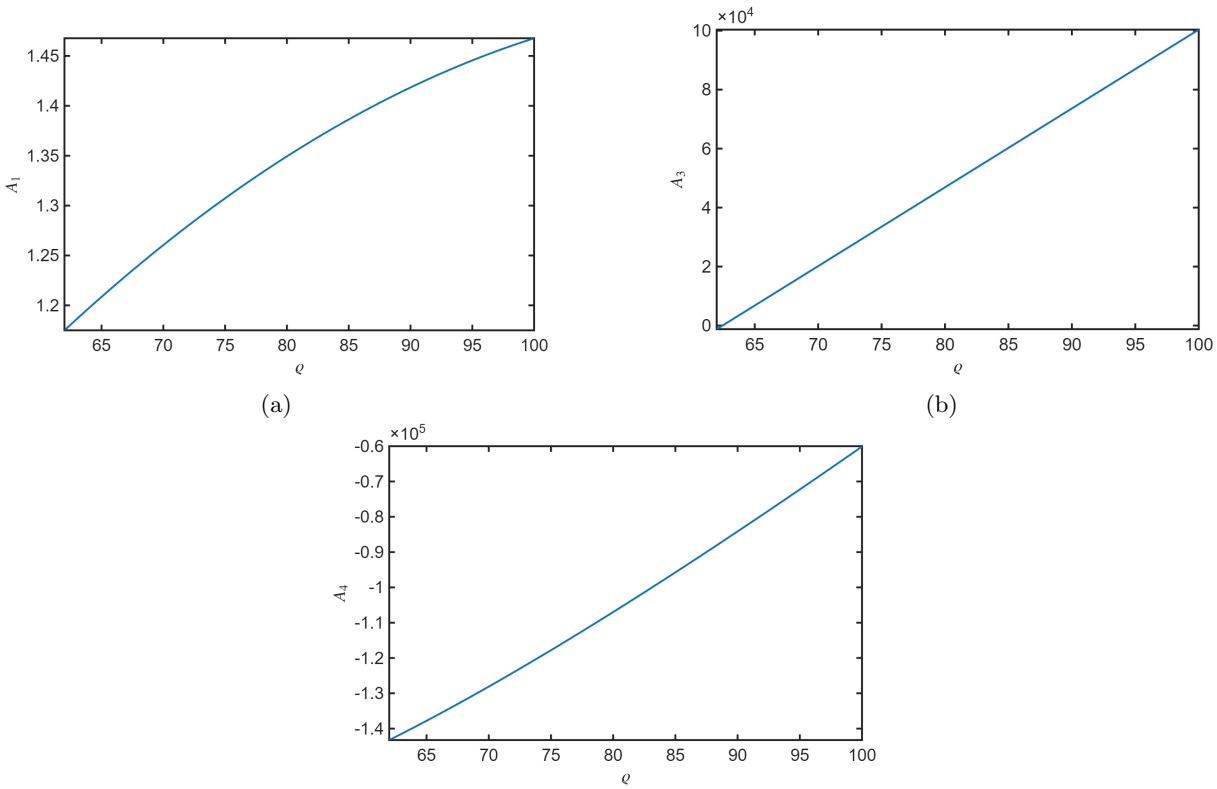

Figure 9: The values of coefficients of cubic polynomial (3.3), (a) A_1 w.r.t viral load $\varrho > \varrho^* = 62.465$, (b) A_3 w.r.t viral load $\varrho > \varrho^* = 62.465$ and (c) the value of $A_4 = f\left(\frac{\Lambda}{\delta(\varrho)}\right)$ w.r.t viral load $\varrho > \varrho^* = 62.465$.

From table 5, we observed that the Routh-Hurwitz conditions in Theorem 3.2 at equilibrium point E^*, $X_1 > 0$, $X_4 > 0$, $X_1X_2 - X_3 > 0$ and $X_1X_2X_3 - X_3^2 - X_4X_1^2 > 0$ at different values of viral load when $\varrho > \varrho^* = 62.465$ when $R_0(\varrho) > 1$. Thus, the Routh-Hurwitz conditions in Theorem 3.2 are validated quantitatively for stability at equilibrium point E^* in table 5 along with the population values in table 4 of model (2.1) at endemic equilibrium level of each compartment corresponding to the specified value of viral load $\varrho > \varrho^* = 62.465$. The fig.10 shows the stability of model (2.1) at endemic point E^* at $\varrho = 75$ when $R_0(\varrho) > 1$.

Table 4: Population values of model (2.1) at endemic equilibrium levels at different values of viral load $\varrho > \varrho^* = 62.465$.

ϱ	S^*	I^*	R^*	S_V^*	I_V^*
62.465	81.1847	1349.73	3135.86	0.0.00020037	42.4998
65	76.9266	1359.55	2971.59	0.000198928	42.4998
75	63.2747	1399.07	2298.47	0.000193309	42.4998
85	53.14	1440.17	1584.19	0.0001877993	42.4998
95	45.2828	1483.22	826.365	0.000182342	42.4998

Table 5: Routh-Hurwitz conditions in Theorem 3.2 at different values of viral load $\varrho > \varrho^* = 62.465$, where $L_1 = X_1X_2 - X_3$ and $L_2 = X_1X_2X_3 - X_3^2 - X_4X_1^2$.

ϱ	X_1	X_4	L_1	L_2
62.465	1.36101	0.00005006	0.619305	0.0311257
65	1.36384	0.00005155	0.6312	0.0326694
75	1.38955	0.00005890	0.699943	0.0413996
85	1.41491	0.00006495	0.762235	0.0497227
95	1.46944	0.00007333	0.87074	0.0641501

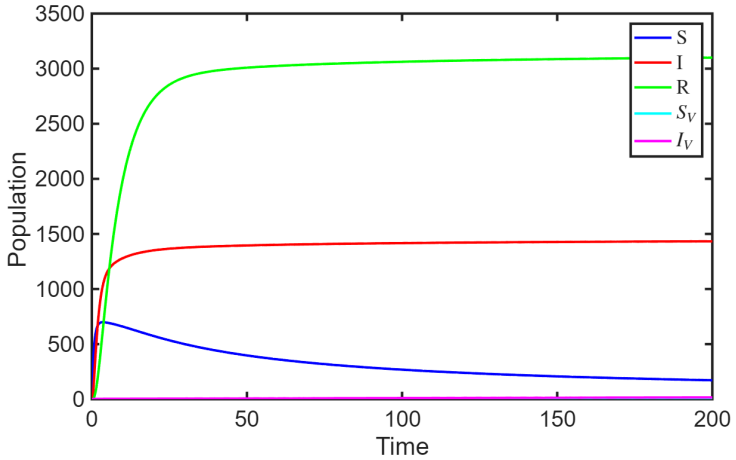

Figure 10: The graph shows the stable behavior of epidemic model (2.1) around endemic equilibrium point E^* w.r.t time when $R_0(\varrho) = 1.1533 > 1$ (at $\varrho = 75$).

4.1. Variation between basic reproduction number $R_0(\varrho)$ and fuzzy reproduction number $R_0^f(\varrho)$ w.r.t viral load ϱ

The behavior of fuzzy basic reproduction number $R_0^f(\varrho)$ and the basic reproduction number $R_0(\varrho)$ for various amounts of parasites ϱ is shown in fig. 11. It can be observed that both are increasing w.r.t parasites ϱ. But as the amount of parasites ϱ approaches to ϱ_M, the basic reproduction number $R_0(\varrho)$ become more than 1 although the fuzzy basic reproduction number $R_0^f(\varrho)$ still remains less than 1. The fuzzy basic reproduction number $R_0^f(\varrho)$ become more than 1 when amount of parasite ϱ exceeds ϱ_M. Thus, the behavior of basic reproduction number $R_0(\varrho)$ is more sensitive as compared to the behavior of fuzzy basic reproduction number $R_0^f(\varrho)$ w.r.t amount of parasite ϱ, which help us to take effective control measures to stabilize the system in early stage when the amount of parasite ϱ below ϱ_M.

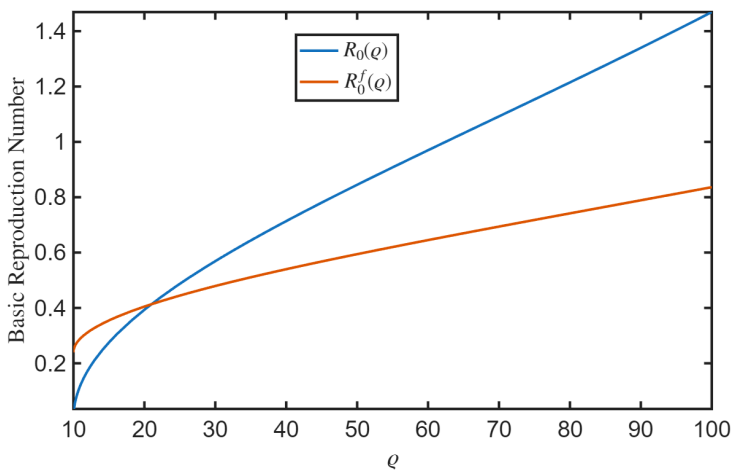

Figure 11: The variation of basic reproduction number $R_0(\varrho)$ and fuzzy basic reproduction number $R_0^f(\varrho)$ for $\varrho_{min} < \varrho < \varrho_M$ w.r.t viral load ϱ.

4.2. Impact of different parameters on $R_0(\varrho)$

Fig.12 illustrates the behavior of $R_0(\varrho)$ w.r.t rate of recovery (α) of human host from the disease at different values of viral load ϱ. It is observed that $R_0(\varrho)$ decreases significantly with increasing movement

of individual from infected class to the susceptible class after recovery even though the amount of viral load ϱ is more than critical value ϱ^* (i.e when $R_0 > 1$). In such a scenario, we can make system stable by increasing the rate of recovery (α) when the amount of viral load ϱ exceeds its critical value ϱ^*.

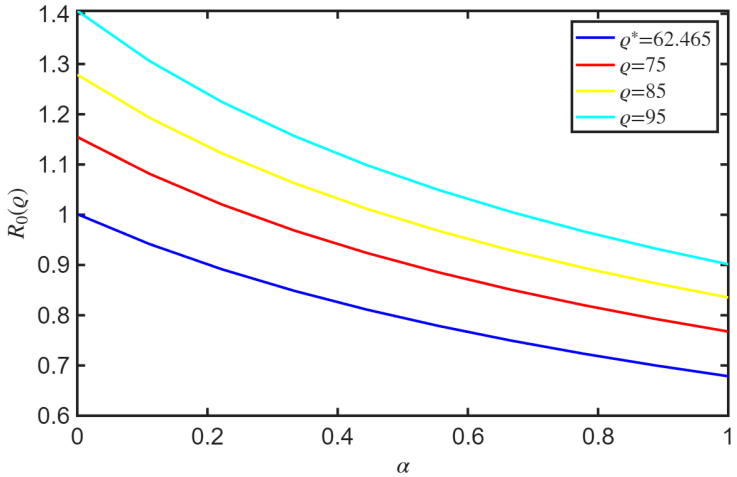

Figure 12: The basic reproduction number $R_0(\varrho)$ w.r.t recovery rate without immunity (α).

Fig.13 illustrates the behavior of $R_0(\varrho)$ w.r.t transmission rate ψ from infected human to susceptible mosquito at different values of viral load ϱ. It is observed that $R_0(\varrho)$ increases significantly with increasing rate of transmission (ψ) from infected individual to susceptible mosquito. It is also noticed that when the amount of viral load ϱ is at it's critical value $\varrho^* = 62.465$ (i.e., where $R_0(\varrho)$ is approximately equal to 1), the value of $R_0(\varrho)$ exceeds 1 w.r.t ψ. This means that when the amount of viral load is below its critical value but the transmission rate from infected individual to susceptible mosquito is being increased then the spreading of the infection of disease excessively in the society.

Fig.14 outline the impact of various parameters on $R_0(\varrho)$ to quantify its role in controlling the spread of infection. From fig.14a, it can be concluded that $R_0(\varrho)$ increases as ϱ increases (keeping α constant). Whereas, $R_0(\varrho)$ decreases if α increases keeping ϱ constant. This reflects that when rate of recovery (α) is fixed but ϱ is increasing at constant rate then it leads to more spreading of infection in the human society. Further, it can be seen that when α and ϱ are at their highest level the infection still exist in the society but at moderate level. Fig.14b, depicts that there is no much effect on $R_0(\varrho)$ by only increasing the value of either ϱ or ψ. But when both the parameters increases simultaneously, then the value of $R_0(\varrho)$ exceeds 1. Thus, in this scenario the system become highly unstable and so the spread of infection at its highest level in the society.

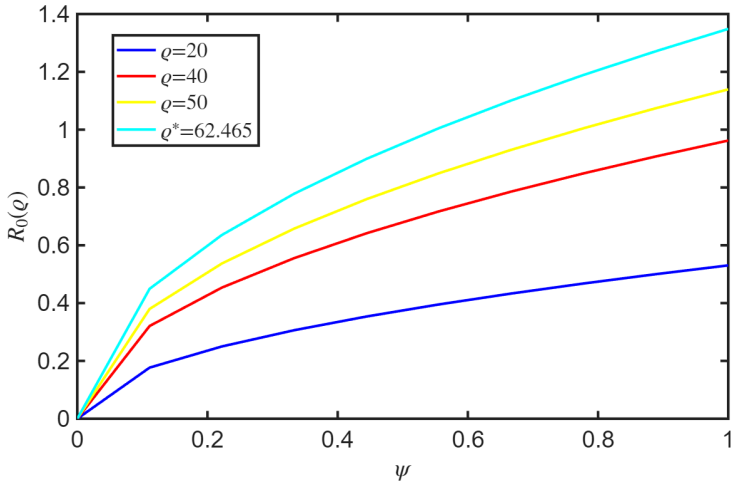

Figure 13: The basic reproduction number $R_0(\varrho)$ w.r.t transmission rate from infected human to susceptible mosquito (ψ).

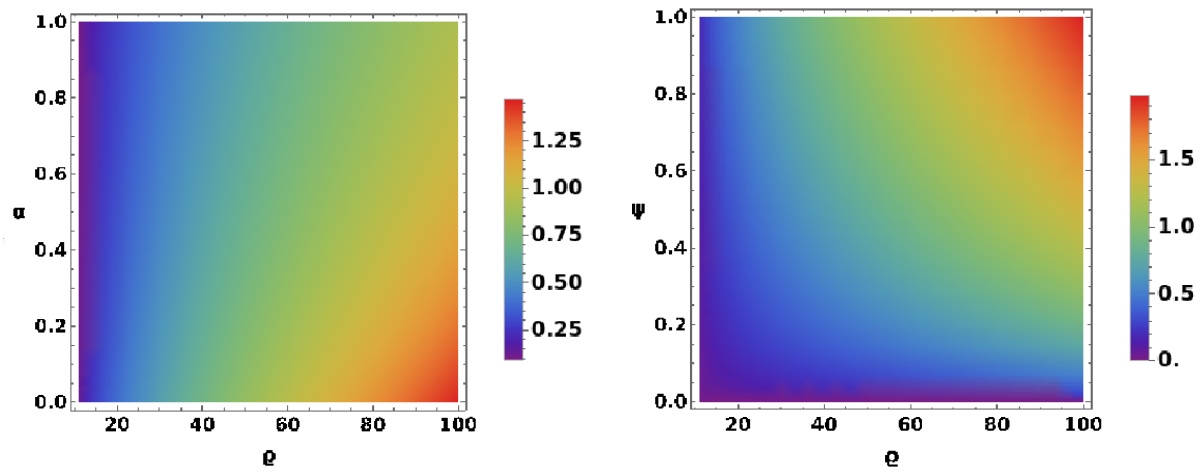

(a) Effect of ϱ and α on $R_0(\varrho)$

(b) Effect of ϱ and ψ on $R_0(\varrho)$.

Figure 14: The graph shows the combined impact of various parameters on $R_0(\varrho)$.

4.3. Impact of parameter on disease prevalence

In this section, we have plotted the infected population with respect to time by taking different values of viral load (ϱ) and recovery rate (α) to see the effect of these parameters on the behavior of disease propagation in the system.

In fig.15, it is observed that on increasing the value of ϱ, the equilibrium level of infected population will also increase, i.e., when the viral load (ϱ) is high, a larger number of people will contract the disease by coming into contact with infected mosquitoes. Hence, there will be an increase in infected individuals in the population. Therefore, it is suggested that measures have to be taken to control the viral load in the society.

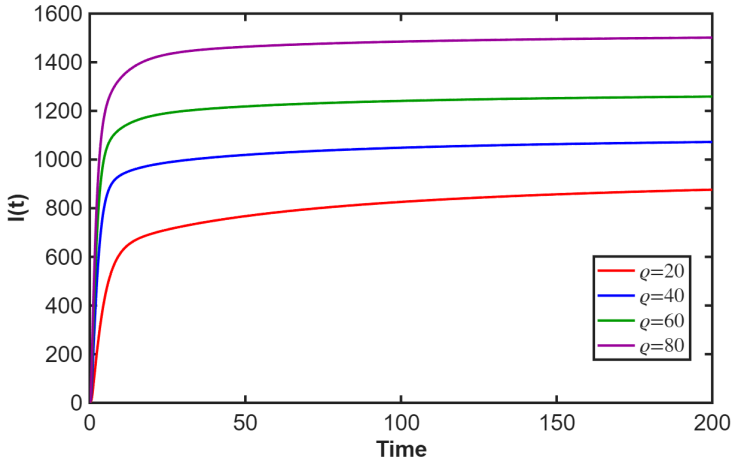

Figure 15: The variation of infected individuals $I(t)$ w.r.t time at different values of viral load ϱ.

From fig.16, we observe that as a value of α increases, the equilibrium level of the infected population will decrease initially, but in the later stage, the increasing value of α does not create so much impact on the decline in the infected population, which is true as the α is the rate of recovery of human hosts from the disease without immunity, and so, the people once recovered without immunity directly move into the susceptible class again and have chances of being infected again.

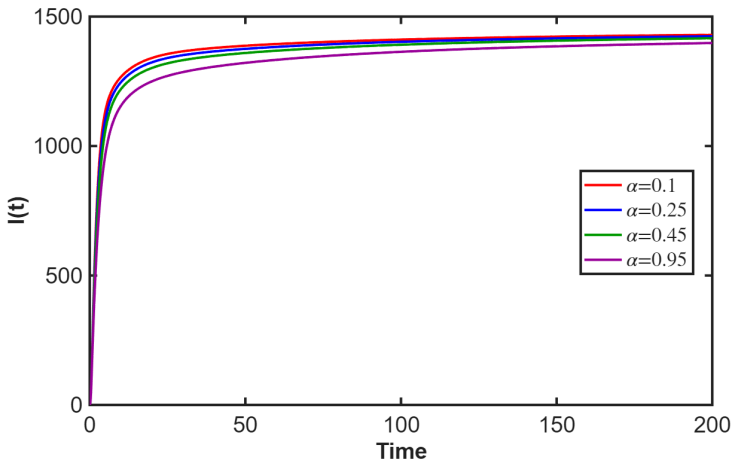

Figure 16: The variation of infected $I(t)$ individuals w.r.t time for different values of α at $\varrho = 75 > \varrho^*$.

4.4. Simultaneous effect of α and ψ on $R_0(\varrho)$ and ϱ^*

In this section we examined the simultaneous effect of parameters (recovery rate (α) and transmission rate (ψ)) on $R_0(\varrho)$ at $\varrho = \varrho^* = 62.465$ and on bifurcation value ϱ^*, provided by eqn. (3.5).

In fig.17, we have plotted the $R_0(\varrho)$ with respect to the transmission rate (ψ) from infected individual to susceptible mosquito and recovery rate (α). We observe that when the transmission rate (ψ) is kept at its highest value and the recovery rate (α) increases, there is a decline in the behavior of $R_0(\varrho)$ and makes it below 1. On keeping recovery rate (α) between 0 to 1 and increasing the transmission rate (ψ), then the $R_0(\varrho)$ would increases significantly. It is concluded that from fig.19, the transmission rate ψ would not make so much burden on the society whenever there is increase in the rate of recovery rate (α).

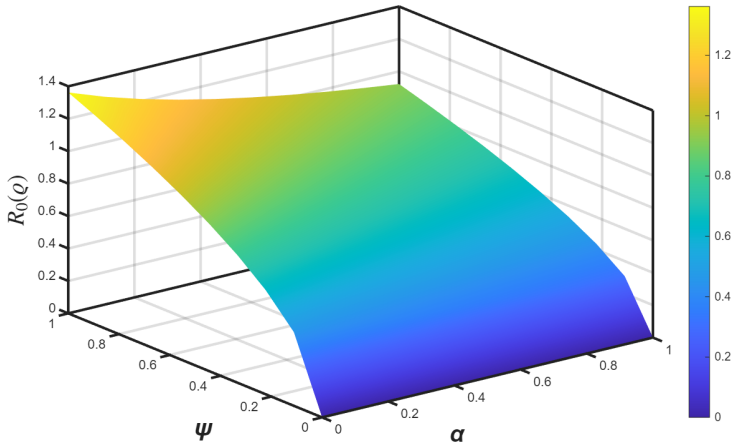

Figure 17: Simultaneous effect of α and ψ on $R_0(\varrho)$ at $\varrho = \varrho^* = 62.465$.

In fig.18, we have plotted the bifurcation value ϱ^* with respect to transmission rate (ψ) from infected individual to susceptible mosquito and recovery rate (α). It can be observed that when both the parameters ψ and α are at their lowest value, the ϱ^* is below 50 and when both are at their highest value, the ϱ^* is approximately 100. Also, when ψ at its minimum value but α at its maximum value than the value of ϱ^* is more than 200. Since, the bifurcation value ϱ^* is that value where $R_0(\varrho)$ become more than 1 when ϱ exceeds ϱ^*. Therefore, it can be inferred from fig.18 that increasing the rate of recovery (α) will increase the value of ϱ^*, thereby boosting system stability.

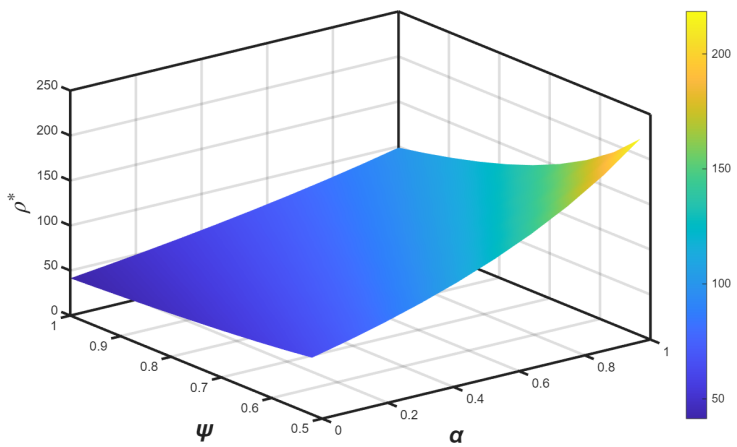

Figure 18: Simultaneous effect of α and ψ on ϱ^*.

4.5. Global sensitivity analysis for $R_0(\varrho)$

The basic reproduction number depends on a number of several uncertain factors. The key parameters associated to basic reproduction number $R_0(\varrho)$ as per our model (2.1), are viral load (ϱ), recovery rate (α) and transmission rate (ψ) from infected human to susceptible mosquito. Thus, to see the effects of these parameters on $R_0(\varrho)$, we therefore perform the global sensitivity analysis of $R_0(\varrho)$. Using suitable uncertainty ranges for each parameter at the same time, we use the Latin Hypercube Sampling (LHS) technique to effectively examine the amount that each of the parameters affects $R_0(\varrho)$ (Marino et al. [31]). Further, to determine the degree of association between $R_0(\varrho)$ and each parameter, we calculate the Partial Rank Correlation Coefficients (PRCCs) for each parameter. The PRCC value fall between -1 and 1. The stronger the correlation between a particular parameter and $R_0(\varrho)$, the higher its absolute PRCC value; a significant change in that parameter is correlated with a similarly significant change in

$R_0(\varrho)$. The sign of the PRCC value indicates the direction of correlation. Positive (or negative) values indicate a positive (or negative) correlation of the parameter with the $R_0(\varrho)$ which implies that the positive (or negative) correlated parameters will increase (or decrease) the value of $R_0(\varrho)$ as positive (or negative) change in the parameters.
We first convert the expression of $R_0(\varrho)$ given in eqn. (3.2) in terms of viral-load ϱ, to determine the extent to which the viral-load influences $R_0(\varrho)$. So, the membership functions $\beta(\varrho)$, $d(\varrho)$, and $r(\varrho)$ from eqn. (2.2), (2.3), and (2.4), respectively, are substituted in eqn. (3.2). We calculate the PRCC values using 1000 simulations per run, assuming that the parameters having uniform distribution. It is evident that from fig.19, measured PRCC values for each parameter, ψ, μ, Λ_V and ϱ show the positive correlation with $R_(\varrho)$. It is observed that viral load ϱ exhibits the strongest positive correlation with the $R_0(\varrho)$. Also, it is noted that (α), (μ_V) and (Λ) show the negative correlation with $R_0(\varrho)$. This means it is important to implement strategies to lower the parametric values of ψ, μ, Λ_V, ϱ; and enhance the parametric values of μ_V, α, Λ, to control the spread of infection in the society.

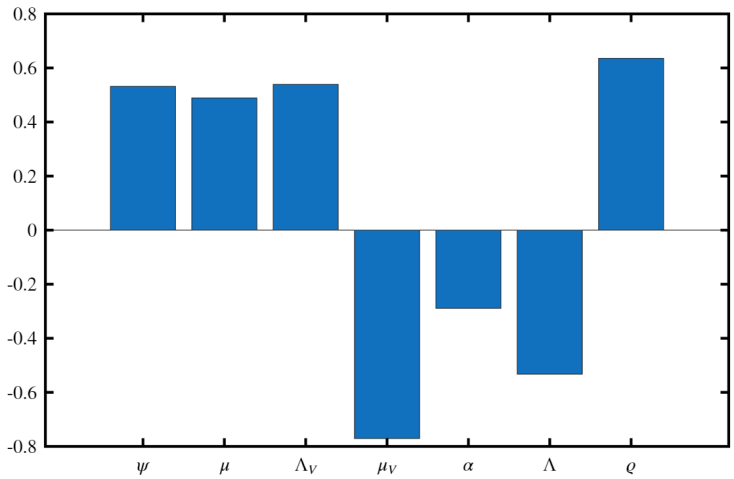

Figure 19: The global sensitivity analysis of basic reproduction number $R_0(\varrho)$.

5. Conclusion

In order to investigate the impact of viral load and immunity (zero or temporary) on the transmission of malaria disease in the society, a compartmental fuzzy SIRSI model has been proposed and is extensively analyzed in the paper. Repeated exposure to malaria, particularly in highly endemic areas, can lead to a type of temporary or "partial" immunity. This doesn't provide sterile protection, meaning the person can still be infected with the malaria parasite, but it can reduce the severity of symptoms and the risk of developing severe, life-threatening disease.

Mathematically, we have derived various analytical results for the system (2.1). Firstly, we have obtained the positivity and boundedness of the solutions of the system (2.1). Steady-state solutions of the system (2.1); the disease-free E_0 as well as the endemic E^* equilibrium points have been obtained. The basic reproduction number $R_0(\varrho)$ in (3.2) has also been evaluated. We have performed stability analysis of the equilibrium points. We have proved that the disease-free equilibrium point E_0 is locally asymptotically stable if $R_0(\varrho) < 1$ and is unstable if $R_0(\varrho) > 1$, which has also been numerically verified as seen in fig.7, and the Routh-Hurwitz criteria given in Theorem 3.1 for the disease-free equilibrium point is validated graphically by fig.6. Under certain conditions, the endemic equilibrium point E^* is proved to be locally asymptotically stable, which has also been numerically validated, as seen in fig.10. We have proved that the endemic equilibrium point E^* is locally asymptotically stable if $R_0(\varrho) > 1$ and satisfies the Routh-Hurwitz criteria in Theorem 3.2, which is validated by table 5. In theorem 3.3, we established fuzzy global stability of system (2.1) by using the approach of graph theory. The bifurcation value has been evaluated as $\varrho^* = 62.465$ at which the $R_0(\varrho)$ becomes 1 and verified graphically in fig.5. The values of $R_0(\varrho) < 1$ for points $\varrho < \varrho^*$ and $R_0(\varrho) > 1$ for points $\varrho > \varrho^*$ are provided by the table 3.

Fig.11 illustrates how the basic reproduction number $R_0(\varrho)$ and fuzzy basic reproduction number $R_0^f(\varrho)$ behave for varying viral load (ϱ) concentrations. We have plotted the basic reproduction number $R_0(\varrho)$ w.r.t. recovery rate without immunity (α) and transmission rate from infected human to susceptible mosquito (ψ), depicted by fig.12 and fig.13, respectively, at different values of viral load ϱ. With the help of contour plots, we have discussed the combined effect of (α, ϱ) and (ψ, ϱ) on $R_0(\varrho)$, which can be seen in fig.14a and fig.14b, respectively. We have plotted the graph of infected individuals $I(t)$ w.r.t (t) time at different values of ϱ in fig.15 and at different values of α in fig.16. With the help of surface plots, we observed the variation in the behavior of $R_0(\varrho)$ and (ϱ^*) w.r.t the α and ψ by fig.17 and fig.18 respectively.

Being already aware of the fact that the basic reproduction number $R_0(\varrho)$ plays a vital role in deciding the dynamics of the disease, we performed global sensitivity analysis of the basic reproduction number $R_0(\varrho)$ that is based on the concepts of Partial Rank Correlation Coefficients (PRCCs) and Latin Hypercube Sampling (LHS), to determine the dependence of $R_0(\varrho)$ on the different model parameters. From fig.19, the transmission rate from infected human to susceptible mosquito (ψ) and viral load (ϱ) play a crucial role for the disease propagation in the society, and so if we need to control the spreading of the disease, our goal must be to control the ψ and ϱ.

In view of the above, we conclude that by implementation of fuzzy logic in epidemic models, we can improve our comprehension of how to develop successful preventative measures by reducing the uncertainty in disease dynamics brought on by differences in viral loads among population.

Funding: The authors declare that no funding has been received.

Data Availability Statement: No data sets were used for the current study. However, we used hypothetical data.

Conflict of interest: Authors declare that there is no Conflict of interest.

References

1. Muhammad Abdy et al. “An SIR epidemic model for COVID-19 spread with fuzzy parameter: the case of Indonesia”. In: Advances in difference equations 2021 (2021), pp. 1–17.
2. Abebe Asale et al. “Community knowledge, perceptions, and practices regard- ing malaria and its control in Jabi Tehnan district, Amhara Region, Northwest Ethiopia”. In: Malaria Journal 20 (2021), pp. 1–13.
3. NTJ Bailey. “The Biomathematics of Malaria (London: Charles Griff)”. In: (1982).
4. Traor´e Bakary, Sangar´e Boureima, and Traor´e Sado. “A mathematical model of malaria transmission in a periodic environment”. In: Journal of biological dynamics 12.1 (2018), pp. 400-432.
5. LC DE Barros, MB Ferreira Leite, and RC Bassanezi. “The SI epidemiological models with a fuzzy transmission parameter”. In: Computers & Mathematics with Applications 45.10-11 (2003), pp. 1619-1628.
6. RC Bassanezi and LC De Barros. “A simple model of life expectancy with subjective parameters”. In: Kybernetes 24.7 (1995), pp. 57-62.
7. Edoardo Beretta, Vincenzo Capasso, and Dario G Garao. “A mathematical model for malaria transmission with asymptomatic carriers and two age groups in the human population”. In: Mathematical biosciences 300 (2018), pp. 87-101.
8. Archana Singh Bhadauria, Sapna Devi, and Nivedita Gupta. “Modelling and analysis of a SEIQR model on COVID-19 pandemic with delay”. In: Modeling Earth Systems and Environment (2022), pp. 1-14.
9. C Castillo Chavez, Z Feng, and W Huang. “On the computation of R_0 and its role on global stability”. In: Mathematical approaches for emerging and re-emerging infection diseases: An introduction 125 (2002), pp. 31-65.
10. Nakul Chitnis, Diggory Hardy, and Thomas Smith. “A periodically-forced mathematical model for the seasonal dynamics of malaria in mosquitoes”. In: Bulletin of mathematical biology 74.5 (2012), pp. 1098-1124.
11. Francis EG Cox. “History of the discovery of the malaria parasites and their vectors”. In: Parasites & vectors 3 (2010), pp. 1-9.
12. Subhashis Das, Prasenjit Mahato, and Sanat Kumar Mahato. “Disease control prey-predator model incorporating prey refuge under fuzzy uncertainty”. In: Modeling Earth Systems and Environment 7.4 (2021), pp. 2149-2166.
13. Rams´es Djidjou-Demasse et al. “Development and analysis of a malaria transmission mathematical model with seasonal mosquito life-history traits”. In: Studies in Applied Mathematics 144.4 (2020), pp. 389-411.
14. Steffen E Eikenberry and Abba B Gumel. “Mathematical modeling of climate change and malaria transmission dynamics: a historical review”. In: Journal of mathematical biology 77.4 (2018), pp. 857-933.
15. Andrea Franceschetti and Andrea Pugliese. “Threshold behaviour of a SIR epidemic model with age structure and immigration”. In: Journal of Mathematical Biology 57.1 (2008), pp. 1-27.

16. Asit K Ghosh, J Chattopadhyay, and PK Tapaswi. "Immunity boosted by low level of exposure to infection in an SIRS model". In: Ecological Modelling 87.1-3 (1996), pp. 227-233.

17. Mini Ghosh. "Mathematical modelling of malaria with treatment". In: Advances in Applied Mathematics and Mechanics 5.6 (2013), pp. 857-871.

18. Andualem Tekle Haringo, Legesse Lemecha Obsu, and Feyissa Kebede Bushu. "A mathematical model of malaria transmission with media-awareness and treatment interventions". In: Journal of Applied Mathematics and Computing 70.5 (2024), pp. 4715-4753.

19. Lars Hviid. "Naturally acquired immunity to Plasmodium falciparum malaria in Africa". In: Acta tropica 95.3 (2005), pp. 270-275.

20. Fasil Adugna Kendie et al. "Prevalence of Malaria among Adults in Ethiopia: A Systematic Review and Meta-Analysis". In: Journal of tropical medicine 2021.1 (2021), p. 8863002.

21. William Ogilvy Kermack and Anderson G McKendrick. "A contribution to the mathematical theory of epidemics". In: Proceedings of the royal society of lon- don. Series A, Containing papers of a mathematical and physical character 115.772 (1927), pp. 700-721.

22. Muhammad Altaf Khan et al. "Stability analysis of an SEIR epidemic model with non-linear saturated incidence and temporary immunity". In: International Journal of Advances in Applied Mathematics and Mechanics 2.3 (2015), pp. 1-14.

23. Ousmane Koutou, Bakary Traor´e, and Boureima Sangar´e. "Mathematical modeling of malaria transmission global dynamics: taking into account the immature stages of the vectors". In: Advances in Difference Equations 2018.1 (2018), p. 220.

24. Jia Li. "Malaria model with stage-structured mosquitoes". In: Math. Biol. Eng 8.3 (2011), pp. 753-768.

25. Michael Y Li, Hal L Smith, and Liancheng Wang. "Global dynamics of an SEIR epidemic model with vertical transmission". In: SIAM Journal on Applied Mathematics 62.1 (2001), pp. 58-69.

26. B Liu. Uncertainty theory 5th Edition. 2014.

27. Baoding Liu. "A survey of entropy of fuzzy variables". In: Journal of uncertain systems 1.1 (2007), pp. 4-13.

28. Baoding Liu and Yian-Kui Liu. "Expected value of fuzzy variable and fuzzy ex- pected value models". In: IEEE transactions on Fuzzy Systems 10.4 (2002), pp. 445-450.

29. Prasenjit Mahato, Subhashis Das, and Sanat Kumar Mahato. "An epidemic model through information-induced vaccination and treatment under fuzzy impreciseness". In: Modeling earth systems and environment 8.3 (2022), pp. 2863-2887.

30. Sandip Mandal, Ram Rup Sarkar, and Somdatta Sinha. "Mathematical models of malaria-a review". In: Malaria journal 10.1 (2011), p. 202.

31. Simeone Marino et al. "A methodology for performing global uncertainty and sensitivity analysis in systems biology". In: Journal of theoretical biology 254.1 (2008), pp. 178-196.

32. K Marsh et al. "Antibodies to blood stage antigens of Plasmodium falciparum in rural Gambians and their relation to protection against infection". In: Transactions of the Royal Society of Tropical Medicine and Hygiene 83.3 (1989), pp. 293-303.

33. Eduardo Massad et al. Fuzzy logic in action: Applications in epidemiology and beyond. Vol. 232. Springer, 2008.

34. Bimal Kumar Mishra and Samir Kumar Pandey. "Fuzzy epidemic model for the transmission of worms in computer network". In: Nonlinear Analysis: Real World Applications 11.5 (2010), pp. 4335-4341.

35. A Mojeeb, E Osman, and AK Isaac. "Simple mathematical model for malaria transmission". In: Journal of Advances in Mathematics and Computer Science 25.6 (2017), pp. 1-24.

36. Prasanta Kumar Mondal et al. "Dynamical behavior of an epidemic model in a fuzzy transmission". In: International Journal of Uncertainty, Fuzziness and Knowledge Based Systems 23.05 (2015), pp. 651-665.

37. Gideon A Ngwa and William S Shu. "A mathematical model for endemic malaria with variable human and mosquito populations". In: Mathematical and computer modelling 32.7-8 (2000), pp. 747-763.

38. A Nwankwo and D Okuonghae. "A mathematical model for the population dynamics of malaria with a temperature dependent control". In: Differential Equations and Dynamical Systems 30.3 (2022), pp. 719-748.

39. OLUYO Temitayo Olabisi and ADENIYI Michael Olaniyi. "The mathematical analysis of malaria transmission: the effect of sanitation". In: Int J Sci Res (IJSR) 7.3 (2018), pp. 236-44.

40. S Olaniyi and OS Obabiyi. "Mathematical model for malaria transmission dynamics in human and mosquito populations with nonlinear forces of infection". In: International journal of pure and applied Mathematics 88.1 (2013), pp. 125-156.

41. Ronald Ross. "Some a priori pathometric equations". In: British medical journal 1.2830 (1915), p. 546.

42. Ronald Ross. "An application of the theory of probabilities to the study of a priori pathometry.—Part I". In: Proceedings of the Royal Society of London. Series A, Containing papers of a mathematical and physical character 92.638 (1916), pp. 204-230.

43. Itishree Sahu and Saumya Ranjan Jena. "SDIQR mathematical modelling for COVID- 19 of Odisha associated with influx of migrants based on Laplace Adomian de- composition technique". In: Modeling Earth Systems and Environment 9.4 (2023), pp. 4031-4040.

44. Zhisheng Shuai and Pauline van den Driessche. "Global stability of infectious disease models using Lyapunov functions". In: SIAM Journal on Applied Mathematics 73.4 (2013), pp. 1513-1532.

45. Boris Shulgin, Lewi Stone, and Zvia Agur. "Pulse vaccination strategy in the SIR epidemic model". In: Bulletin of mathematical biology 60.6 (1998), pp. 1123-1148.

46. SY Tchoumi et al. "Malaria and COVID-19 co-dynamics: A mathematical model and optimal control". In: Applied mathematical modelling 99 (2021), pp. 294-327.

47. SY Tchoumi et al. "Malaria and malnutrition in children: A mathematical model". In: Franklin Open 3 (2023), p. 100013.

48. Bakary Traor´e, Ousmane Koutou, and Boureima Sangar´e. "A global mathematical model of malaria transmission dynamics with structured mosquito population and temperature variations". In: Nonlinear Analysis: Real World Applications 53 (2020), p. 103081.

49. Bakary Traor´e, Boureima Sangar´e, and Sado Traor´e. "A mathematical model of malaria transmission with structured vector population and seasonality". In: Journal of Applied Mathematics 2017.1 (2017), p. 6754097.

50. Julius Tumwiine, JYT Mugisha, and Livingstone S Luboobi. "A mathematical model for the dynamics of malaria in a human host and mosquito vector with temporary immunity". In: Applied mathematics and computation 189.2 (2007), pp. 1953-1965.

51. Muhammad Asad Ullah et al. "Analysis and interpretation of a novel malaria transmission mathematical model with socioeconomic structure". In: Nonlinear Dynamics 113.10 (2025), pp. 12399-12418.

52. Pauline Van den Driessche and James Watmough. "Reproduction numbers and sub-threshold endemic equilibria for compartmental models of disease transmission". InMathematical biosciences 180.1-2 (2002), pp. 29-48.

53. Renu Verma, SP Tiwari, and Ranjit Kumar Upadhyay. "Dynamical behaviors of fuzzy SIR epidemic model". In: Proceedings of the Conference of the European Society for Fuzzy Logic and Technology. Springer. 2017, pp. 482-492.

54. Lisa J White et al. "The role of simple mathematical models in malaria elimination strategy design". In: Malaria journal 8.1 (2009), p. 212.

55. WHO. "World Malaria Report 2024". In: https://www.who.int/teams/global-malaria-programme/reports/world-malaria-report-2024 (2024).

56. Lotfi A Zadeh. "Fuzzy sets". In: Information and control 8.3 (1965), pp. 338-353.

Sakshi Singh,
Department of Mathematics,
Jaypee Institute of Information Technology,
India.
E-mail address: sakshi965479@gmail.com

and

Shashank Goel,
Department of Mathematics,
Jaypee Institute of Information Technology,
India.
E-mail address: goel.shashank25@gmail.com

and

Alka Tripathi,
Department of Mathematics,
Jaypee Institute of Information Technology,
India.
E-mail address: alka.choubey@gmail.com